Journal of Applied Analysis and Computation
Volume 12, Number 2, April 2022, 533–550
Website:http://www.jaac-online.com
DOI:10.11948/20210195

CONSTRUCTION OF NEW TRAVELING WAVE SOLUTIONS FOR THE (2+1) DIMENSIONAL EXTENDED KADOMTSEV-PETVIASHVILI EQUATION*

M. E. Elbrolosy[1,2,†] and A. A. Elmandouh[1,3]

Abstract This work is interested in constructing traveling wave solutions for the (2+1)-dimensional extended Kadomtsev–Petviashvili equation that is utilized as a model for the surface waves and internal waves in straits or channels. Based on the bifurcation analysis of the traveling wave system, we use the conserved quantity to construct some new bounded traveling wave solutions such as periodic and solitary solutions in addition to some unbounded novel wave solutions. Some of the new solutions and their corresponding orbits are clarified graphically. Moreover, we examine numerically the dynamical behaviour for the perturbed (2+1)-dimensional extended Kadomtsev–Petviashvili equation by adding a perturbed periodic term.

Keywords Bifurcation, traveling wave solutions, (2+1)-dimensional Kadomtsev–Petviashvili equation.

MSC(2010) 35Q53, 35C07, 35Q92.

1. Introduction

In recent few decades, the wide applications of nonlinear evolution equations(NLEEs) have become an important research area for the interested in the study of applied sciences aiming to seek exact soliton solutions. These applications mostly appear in various fields such as fluid dynamics, optical fibers, water waves, plasma, nuclear physics and biological systems. NLEEs are considered in finite dimensions such as (1+1), (2+1) and (3+1)-dimensions. Kadomtsev-Petviashvili equation (KPe) is a significant one of those NLEEs. The KPe appears in various fields especially in the nonlinear dynamical systems, such as ferromagnetic media, water waves and multi-component plasmas. There are several techniques of integration that were established in literature. In [9] the (2+1)-dimensional Camassa-Holm KPe has been studied utilizing of the G'/G method, the exponential function method and the ansatz method. In [10, 11, 36, 37] the (3+1)-dimensional extended KPe has

†The corresponding author. Email: melborolosy@kfu.edu.sa(M. E. Elbrolosy)
1Department of Mathematics and Statistics, College of Science, King Faisal University, P. O. Box 400, Al-Ahsa 31982, Saudi Arabia
2Department of Mathematics, Faculty of Science, Tanta University, Tanta 31527, Egypt
3Department of Mathematics, Faculty of Science, Mansoura University, Mansoura 35516, Egypt
*The authors acknowledge the Deanship of Scientific Research at King Faisal University for the financial support under Nasher Track (No. 206139).

been studied with power law nonlinearity appearing in the multi-component plasmas study. Based on a computerized symbolic computation and extended variable coefficient homogeneous balance method, the dynamics of solitons and nonlinear waves in plasmas and superfluids have been described for the (3+1)-dimensional KPe in [25]. In [45] a modified three-soliton method has been proposed and applied to the (2+1)-dimensional KPe. In [6] the multiple Exp-function method has been applied to construct multiple wave solutions for the (3 +1)-dimensional generalized B-type KPe. A Shallow water wave equation in [3, 24], has been modeled by (2+1)-dimensional Gardner-KPe to obtain soliton and other solutions. The multiple exp-function method has been applied to explore the shape nature of anti-kink solutions of a (3+1)-dimensional B-type KPe in [8]. The Lie symmetry method has been applied to the logarithmic-KP equation in [38]. A lattice Boltzmann method has been proposed in [39] to simulate the solitons of the KPe. In [46] a Hirota bilinear differential equation method has been proposed to a (3+1)-dimensional generalized KPe and two classes of lump solutions have been derived. In [33] the authors used F-expansion method and the generalized extended tanh method to develop solitary waves solutions of both KPe and modified KPe. Lump solutions to a (2+1)-dimensional extended KPe have been presented in [30]. More recently, generalized bilinear method has been used for (3+1)-dimensional KP-Boussinesq-like equation to study the dynamics of lump solutions in [34]. The Hirota bilinear method has been investigated in [1, 22] for (2+1)-dimensional extended KPe modeling the surface and internal waves. In [35] a modification form of extended auxiliary equation mapping method has been applied in a generalized KP modified equal width-Burgers. By a symbolic calculation technique, the lump-kink solutions and multiple-soliton have been obtained in [23] for generalized (3+1)-dimensional KPe. In [12] multi-wave solutions for Hirto equation are obtained utilizing three powerful function techniques. The extension exponential rational function method has been applied successfully in [13] to build some novel traveling wave solution for the higher Sharma-Tasso-Olver equation. Some traveling wave solutions nonlinear propagation of Kundu–Eckhaus dynamical model were introduced in [14] using using logarithmic transformation and function method. In Ref [15] authors introduced multi- wave solutions for the hydrodynamics Zakharov- Kuznetsov model. Extra papers dealing with these types of equations can be found in [4, 5, 7, 29, 40–44].

In this paper, we consider a (2+1)-dimensional extended KPe:

$$(u_t + 6uu_x + u_{xxx})_x - u_{yy} + \alpha u_{tt} + \beta u_{ty} = 0, \tag{1.1}$$

where α, β are arbitrary constants. We will apply the bifurcation method which has been successfully utilized to construct traveling wave solutions for different problems (see, e.g., [16–21, 26–28, 31, 32, 47]). Several reasons are motivating us to apply the bifurcation method to construct traveling wave solutions for a given PDE. One of the most important reasons is the ability to determine the type of the solutions through the kind of the corresponding orbits before finding the solutions. For instance, the existence of periodic orbits, homoclinic orbits, and smooth heteroclinic orbits for traveling wave systems refers to periodic wave solutions, smooth solitary solutions, and smooth kink wave solutions, or oscillatory traveling wave solutions for partial differential equations, respectively. Also, it has some advantages which will be outlined in the text for suitability.

The work in the following is organized as: Section 2 presents analysis of bifurcation and phase portrait of the planar dynamical system corresponding to Eq. (1.1).

Section 3 is concerned with constructing traveling wave solutions for Eq. (1.1) by applying the bifurcation analysis. Graphical representations are given in Section 4. Section 5 contains the study of the dynamical behaviour for the perturbed (2+1)-dimensional extended Kadomtsev– Petviashvili equation due to the adding a perturbed periodic term. Section 6 is a conclusion of the work.

2. Bifurcation and phase portrait

We consider the traveling wave transformation

$$u = \psi(\eta), \qquad \eta = kx + ly - \omega t, \tag{2.1}$$

where k, l are constants referring the direction cosine of the propagation of traveling wave velocity ω in the plane xy. Inserting the transformation (2.1) into Eq. (1.1), we get

$$k^4\psi'''' + [\alpha\omega^2 - l^2 - \omega(k + l\beta)]\psi'' + 6k^2\psi\psi'' + 6k^2{\psi'}^2 = 0, \tag{2.2}$$

where $'$ refers to the derivative with respect to η. Integrating Eq. (2.2) twice with respect to η and setting the first integration constant equals to zero, we obtain

$$\psi'' + \frac{3}{k^2}\psi^2 + \gamma\psi = \rho, \tag{2.3}$$

where ρ is an arbitrary constant and γ is given by

$$\gamma = \frac{\alpha\omega^2 - \omega(k - l\beta) - l^2}{k^4}. \tag{2.4}$$

Eq. (2.3) can be presented as a planar dynamical system in the form

$$\begin{aligned} \psi' &= z, \\ z' &= \frac{-3}{k^2}\psi^2 - \gamma\psi + \rho. \end{aligned} \tag{2.5}$$

System (2.5) is named a traveling wave system. System (2.5) is a conservative system because $\frac{\partial\psi'}{\partial\psi} + \frac{\partial z'}{\partial z} = 0$. Moreover, it is a Hamilton system because is derived from the canonical Hamilton equations $\psi' = \frac{\partial H}{\partial\psi}, z' = -\frac{\partial H}{\partial\psi}$, where H is a Hamiltonian function and it takes the form

$$H = \frac{z^2}{2} + \frac{\psi^3}{k^2} + \frac{\gamma}{2}\psi^2 - \rho\psi. \tag{2.6}$$

In physics, the Hamiltonian shown in Eq. (2.6) describes one dimension motion of a particle taking place as a result of the potential forces that are derived from the potential function

$$V(\psi) = \frac{\psi^3}{k^2} + \frac{\gamma\psi^2}{2} - \rho\psi. \tag{2.7}$$

Due to the Hamiltonian shown in Eq. (2.6) does not explicitly rely on the independent variable η that plays the role of the time in mechanics and so, the Hamiltonian (2.6) is a conserved quantity. Thus, we have

$$\frac{z^2}{2} + \frac{\psi^3}{k^2} + \frac{\gamma}{2}\psi^2 - \rho\psi = h, \tag{2.8}$$

where h is a constant.

The study of the bifurcation of the traveling wave system (2.5) represents significant role in constructing and explaining the traveling wave solution for Eq. (1.1). Assuming $u=\psi(\eta)$ is a continuous solution for Eq. (1.1) for $\eta\in\mathbb{R}$ with $\lim_{\eta\to+\infty}\psi(\eta)=\nu_1$ and $\lim_{\eta\to-\infty}\psi(\eta)=\nu_2$. Hence, u is named a solitary wave solution if $\nu_1=\nu_2$, while it is a kink(or anti-kink) wave solution if $\nu_1\neq\nu_2$. Moreover, there is a relation between the type of the orbits and the classification of the wave solution. For instance, the solitary wave solution and kink (anti-kink) wave solutions for Eq. (1.1) are associated with the homoclinic and hetroclinic orbits for the system (2.5), respectively. Also, the existence of periodic orbit for system (2.5) refers the presence of periodic traveling wave solution. Consequently, this motivates us to study the bifurcation of system (2.5) in order to be able to classify the solutions into solitary waves, breaking waves, kink (anti-kink) waves and periodic waves depending on the type of the orbits for the system (2.5).

To investigate the bifurcation and phase portrait for the dynamical system shown in Eq. (2.5), we find its equilibrium points and study their nature. Clearly, we set $\psi'=0$ and $z'=0$ to find the equilibrium points and consequently, the equilibrium points lie on $\psi-$ axis and satisfies the quadratic equation $\frac{3\psi^2}{k^2}+\gamma\psi-\rho=0$. Thus, we have the following possibilities:

i. If $\gamma^2k^2+12\rho<0$, there is no equilibrium point.
ii. If $\gamma^2k^2+12\rho=0$, there is a double equilibrium point $E_1=\left(\frac{-\gamma k^2}{6},0\right)$.
iii. If $\gamma^2k^2+12\rho>0$, the equilibrium points are $E_2=\left(\frac{-\gamma k^2+|k|\sqrt{\gamma^2k^2+12\rho}}{6},0\right)$ and $E_3=\left(\frac{-\gamma k^2-|k|\sqrt{\gamma^2k^2+12\rho}}{6},0\right)$.
Without loss of generality we can assume hencforth that k is positive.

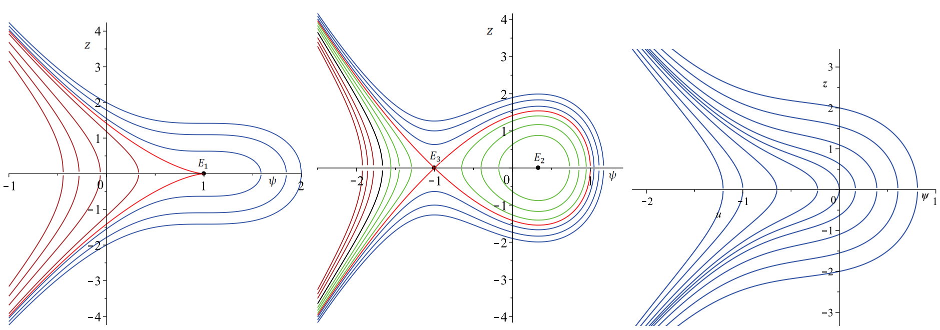

(a) $k=1,\gamma=-6,\rho=-3$ (b) $k=1,\gamma=2,\rho=1$ (c) $k=1,\gamma=2,\rho=-1$

Figure 1. Phase portrait for the planar dynamical system (2.5). The solid circles indicate to the equilibrium points.

To specify the nature of the equilibrium points E_i in view of the theory of planar dynamical systems, we calculate the eigenvalues of the Jacobian matrix of system (2.5) evaluated at the equilibrium $(\psi_0,0)$ and they are

$$\lambda_{1,2}=\pm\sqrt{\frac{-6\psi_0}{k^2}-\gamma}. \tag{2.9}$$

Therefore, the equilibrium point E_1 will be a cusp since the eigenvalues (2.9) at E_1 are zeros and the Poincaré index of that point is 0. The phase portrait for this case is illustrated by Fig. 1(a) for different values of the parameter h and the point E_1 is indicated as a black point. On the other side, the eigenvalues (2.9) at E_2 and E_3 will be $\pm\sqrt{-\frac{\sqrt{\gamma^2 k^2+12\rho}}{k}}$ and $\pm\sqrt{\frac{\sqrt{\gamma^2 k^2+12\rho}}{k}}$ respectively. So, the equilibrium point E_2 is a center point while E_3 is a saddle point and thus, the phase portrait for this case is clarified by Fig. 1(b) for different values of the parameter h and equilibrium points E_2 and E_3 are outlined by two solid points.

It is clear that the space surface $\mathcal{C}_0 = \{(\rho, k, \rho) \in \mathbb{R}^3, \gamma^2 k^2 + 12\rho = 0\}$ splits the 3D parameter space into two zones. The related parameter bifurcation sets are

$$
\begin{aligned}
\mathcal{C}_0 &= \{(\rho, k, \gamma) \in \mathbb{R}^3, \gamma^2 k^2 + 12\rho = 0\},\\
\mathcal{C}_+ &= \{(\rho, k, \gamma) \in \mathbb{R}^3, \gamma^2 k^2 + 12\rho > 0\},\\
\mathcal{C}_- &= \{(\rho, k, \gamma) \in \mathbb{R}^3, \gamma^2 k^2 + 12\rho < 0\}.
\end{aligned}
\tag{2.10}
$$

To clarify the parameter bifurcation sets intuitively, let us fix the parameter γ to a fixed value γ_0 and hence the bifurcation boundary takes the form

$$
L : \rho = -\frac{\gamma_0^2 k^2}{12}. \tag{2.11}
$$

This boundary curve splits the $k\rho$-plane into two disjoint regions as it is outlined by Fig. 2.

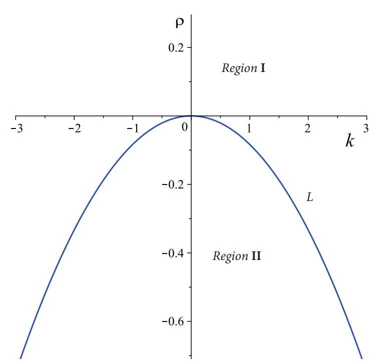

Figure 2. Bifurcation boundary on the $k\rho$-plane for a fixed value of γ.

3. Constructing traveling wave solutions using a conserved quantity

Now, we are going to construct some traveling wave solutions for Eq. (1.1) taking into account the bifurcation analysis. Entering the first equation in Eq. (2.5) into Eq. (2.8) and separating the variables, we obtain

$$
\frac{\sqrt{2}}{k}\mathrm{d}\eta = \frac{\mathrm{d}\psi}{\sqrt{R_3(\psi)}}, \tag{3.1}
$$

where

$$R_3(\psi) = -\psi^3 - \frac{k^2\gamma}{2}\psi^2 + k^2\rho\psi + k^2 h. \tag{3.2}$$

To integrate both sides of Eq. (3.1), the range of the parameters γ, ρ, k, and h is demanded due to the different values of these parameters will imply to different wave solutions. Hence, the key step for integrating Eq. (3.1) is finding this range of those parameters. There are two methods used to detect these ranges of parameters such as a bifurcation analysis and the complete discrimination system function for $R_3(\psi)$. The application of bifurcation theory is more significant and has some advantages over the other method. It gives the range of the parameters and can also be employed to classify the types of traveling wave solutions through the type of the the orbits without calculating the solutions. Based on the physical meaning of the problem under consideration, we restrict ourselves in construction real traveling wave solutions for Eq. (1.1). Hence, we only consider certain intervals for ψ for which $R_3(\psi) > 0$. Furthermore, the construction of all possible traveling wave solutions for Eq. (1.1) requires to specify the type of the orbits for system (2.5) either it is bounded or unbounded for different values of the energy h. Hence, it is more suitable to introduce the proposition

Proposition 3.1. *The traveling wave system* (2.5) *has only two types of bounded orbits which are the periodic orbit in green and homoclinic orbit in red as illustrated by Fig. 1(b). While the other orbits are unbounded orbits as outlined in Fig. 1.*

Now, we calculate the values of the energy h at the equilibrium points $E_i, i = 1, 2, 3$, we have

$$\begin{aligned} h_1 &= -\frac{1}{216}k^4\gamma^3, \\ h_2 &= \frac{k}{216}(k\gamma - \sqrt{k^2\gamma^2 + 12\rho})(k^2\gamma^2 - k\gamma\sqrt{k^2\gamma^2 + 12\rho} + 24\rho), \\ h_3 &= \frac{k}{216}(k\gamma + \sqrt{k^2\gamma^2 + 12\rho})(k^2\gamma^2 + k\gamma\sqrt{k^2\gamma^2 + 12\rho} + 24\rho). \end{aligned} \tag{3.3}$$

Thus, we integrate Eq. (3.1) along these bounded and unbounded orbits individually.

3.1. Expressions of bounded traveling waves of system (2.5)

According to the proposition 3.1, only when $(\rho, k, \gamma) \in \mathcal{C}_+$, there exist bounded traveling wave solutions. These solutions are periodic waves and solitary wave because they corresponds periodic orbits and homoclinic orbit, respectively.

3.1.1. Periodic waves

On the level $h \in]h_2, h_3[$, there is a family of periodic orbits in green around the center point E_2 which is surrounded by the homoclinic orbit in red as outlined by Fig. 1(b). Any orbit of this family cuts $\psi-$axis in three points and this shows the polynomial $R_3(\psi)$ has three simple real roots. Thus, $R_3(\psi) = (\psi - r_1)(\psi - r_2)(r_3 - \psi)$, where r_1, r_2, r_3 are real parameters with $r_1 < r_2 < \psi < r_3$. Let us assume the period of this closed curve is $2T$ and $\psi(0) = r_2$. Thus, Eq. (1.1) becomes

$$\int_{r_2}^{\psi} \frac{dq}{\sqrt{(q - r_1)(q - r_2)(r_3 - q)}} = \frac{\sqrt{2}}{k}\int_0^{\eta} d\eta. \tag{3.4}$$

Eq. (3.4) gives the periodic wave solution in the form

$$u(\eta)=\psi(\eta)=\frac{r_2(r_3-r_1)-r_1(r_3-r_2)\mathrm{sn}^2(\Omega_1\eta,k_1)}{(r_3-r_1)\mathrm{dn}^2(\Omega_1\eta,k_1)},\quad -T<\eta<T, \tag{3.5}$$

where $\Omega_1=\frac{1}{k}\sqrt{\frac{r_3-r_1}{2}}, k_1=\sqrt{\frac{r_3-r_2}{r_3-r_1}}$. The solution (3.5) is a new periodic wave solution for Eq. (1.1) with period $\frac{2}{k_1}K(k_1)$, where $K(k_1)$ is a complete elliptic integral of the first kind [2].

3.1.2. Solitary waves

When the value of the energy of the system (2.5) equals the value of the energy at the saddle point E_3, i.e., $h=h_3$, there is an orbit in red passing through the saddle point E_3, see Fig. 1(b). This orbit cuts the $\psi-$ axis in two points and this proves the polynomial $R_3(\psi)$ has three real roots; one is simple and the other is double at E_3. Thus, the polynomial $R_3(\psi)$ can be written in the form $R_3(\psi)=(\psi-r_4)^2(r_5-\psi)$, where $r_4=\frac{-\gamma k^2-k\sqrt{\gamma^2k^2+12\rho}}{6}$ and $r_4<\psi<r_5$. Let us assume $\psi(0)=r_5$ and Insert $R_3(\psi)$ into Eq. (3.1) and integrate both sides, we obtain

$$\int_{r_5}^{\psi}\frac{dq}{(q-r_4)\sqrt{r_5-q}}=\frac{\sqrt{2}}{k}\int_0^{\eta}d\eta. \tag{3.6}$$

Eq. (3.6) gives

$$u(\eta)=\psi(\eta)=r_4+\frac{2(r_5-r_4)}{1+\cosh\Omega_2\eta},-\infty<\eta<\infty, \tag{3.7}$$

where $\Omega_2=\frac{\sqrt{2(r_5-r_4)}}{k}$.

3.2. Expressions for unbounded traveling waves of system (2.5)

In this section, we construct unbounded traveling waves of the system (2.5) along energy curves for distinct values of the energy. We consider the following cases, individually

Case 3.1: Let us assume $(\rho,k,\gamma)\in\mathcal{C}_0$, there are unbounded orbits according to the value of the energy h.

1. If the value of the energy does not equal to the value of the energy at the cusp point, i.e., $h\neq h_1$, the system (2.5) has two families of unbounded orbits in blue and in brown $\{H(\psi,z)=h,h\neq h_1\}$, see Fig. 1(a). A single orbit of these families whether it is in blue or brown intersects $\psi-$axis in one point and this proves the the polynomial $R_3(u)$ has one real root and two conjugate complex roots. Thus, it can be written as $R_3(\psi)=(r_6-\psi)(\psi-c_1)(\psi-\bar{c_1})$, where $-\infty<\psi<r_6$ and let $\psi(-\infty)=0$. We use the last formula for $R_3(\psi)$ and Eq. (3.1), we get

$$\int_{-\infty}^{\psi}\frac{dq}{\sqrt{(r_6-q)(q-c_1)(q-\bar{c_1})}}=\frac{\sqrt{2}}{k}\int_0^{\eta}d\eta, \tag{3.8}$$

for $\eta > 0$. Eq. (3.8) gives

$$u(\eta) = \psi(\eta) = r_4 + A_1 - \frac{2A_1}{1 - \operatorname{cn}(\Omega_3 \eta, k_2)}, \quad 0 < \eta < \eta_1 \tag{3.9}$$

where $\Omega_3 = \frac{\sqrt{2A_1}}{k}, k_2 = \sqrt{\frac{A_1 - \Re c_1 + r_6}{2A_1}}, A_1^2 = [\Re c_1 - r_6]^2 + \Im^2 c_1$ and $\eta_1 = \int_0^{\pi/2} \frac{dt}{\sqrt{1 - k_2^2 \sin^2 t}}$.

2. If the energy of the system equals the value of the energy at the cusp, the system has another unbounded orbit in red as outlined by Fig. 1(a). This orbit intersects the $\psi-$axis in a single point which is the equilibrium point E_1. This proves the polynomial $R_3(\psi)$ has three multiple roots and so it is written in the form $R_3(\psi) = -\left(\psi + \frac{k^2\gamma}{6}\right)^3$, where $-\infty < \psi < -\frac{k^2\gamma}{6}$. Let us assume $\psi(0) = -\infty$. Taking into account the upper branch of this orbit and Insert this formula for $R_3(\psi)$ into Eq. (3.1) and integrating both sides, we get

$$u(\eta) = \psi(\eta) = -\frac{k^2\gamma}{6} - \frac{2k^2}{\eta^2}, \quad \eta > 0. \tag{3.10}$$

Case 3.2: We consider the case $(\rho, k, \gamma) \in \mathcal{C}_+$. The phase portrait for the system (2.5) in this case is described by Fig. 1(b). The system has some family of unbounded orbits for different values of h. Based on different values of the energy h, we construct unbounded traveling wave solutions for system (2.5). Let us consider them separately:

1. On the energy level which is greater than the energy at the saddle point E_3, there is a family of orbits, $H(\psi, z) = h, h > h_3\}$, in blue as outlined by Fig. 1(b). Any member of this family cuts $\psi-$axis in one point and this shows the polynomial $R_3(\psi)$ has only one real zero and the others are two conjugate complex. Thus, it can be written in the form $R_3(\psi) = (r_7 - \psi)(\psi - c_2)(\psi - \bar{c_2})$, where $-\infty < \psi < r_7$. We postulate $\psi(0) = -\infty$. Inserting the last formula for $R(\psi)$ into Eq. (1.1), we obtain

$$\int_{-\infty}^{\psi} \frac{dq}{\sqrt{(r_7 - q)(q - c_2)(q - \bar{c_2})}} = \frac{\sqrt{2}}{k} \int_0^{\eta} d\eta, \tag{3.11}$$

for $\eta > 0$. Eq. (3.11) gives

$$u(\eta) = \psi(\eta) = r_7 + A_2 - \frac{2A_2}{1 - \operatorname{cn}(\Omega_4 \eta, k_3)}, \quad 0 < \eta < \eta_2, \tag{3.12}$$

where $\Omega_4 = \frac{\sqrt{2A_2}}{k}, k_3 = \sqrt{\frac{A_2 - \Re c_2 + r_7}{2A_2}}, A_2^2 = [\Re c_2 - r_7]^2 + \Im^2 c_2$ and $\eta_2 = \frac{4}{\Omega_4} K(k_3)$, where $K(k_3)$ is a complete elliptic integral of the first type [2].

2. If $h \in]h_2, h_3[$, there is two families of orbits in green as outlined by Fig. 1(b). One of them is a periodic family around the center point E_2, it is bounded and it is considered in sub subsection 3.1.1. While the other one has the parabolic shape and it is unbounded and so it is consider here. The polynomial $R_3(\psi)$ is expressed as $R_3(\psi) = (r_1 - \psi)(r_2 - \psi)(r_3 - \psi)$. We assume $\psi(0) = -\infty$

and $-\infty < \psi < r_1 < r_2 < r_3$. Inserting the last formula for $R_3(\psi)$ into the differential form (3.1) and integrating both sides, we obtain

$$\int_{-\infty}^{\psi} \frac{dq}{\sqrt{(r_1-q)(r_2-q)(r_3-q)}} = \frac{\sqrt{2}}{k}\int_0^{\eta} d\eta, \tag{3.13}$$

for $\eta > 0$. Thus, we have

$$u(\eta) = \psi(\eta) = r_3 - (r_3 - r_1)\mathrm{ns}^2(\Omega_5\eta, k_4), \quad 0 < \eta < \eta_3, \tag{3.14}$$

where $\Omega_5 = \frac{1}{k}\sqrt{\frac{r_3-r_1}{2}}, k_4 = \sqrt{\frac{r_3-r_2}{r_3-r_1}}$, and $\eta_3 = \frac{4}{\Omega_5}K(k_4)$, where $K(k_4)$ is a complete elliptic integral of the first kind [2].

3. If $h \in]-\infty, h_2[$, there is a family of unbounded orbits with hyperbolic shape in brown color for the dynamical system (2.5). A single orbit of this family cuts $\psi-$ axis in one point and this proves the polynomial (3.2) has only one real root. Thus, the polynomial (3.2) can be written in the form $R_3(\psi) = (r_8 - \psi)(\psi - c_3)(\psi - \bar{c_3})$, where $-\infty < \psi < r_8$ and we assume $\psi(0) = -\infty$. Entering the last expression for $R_3(\psi)$ into Eq. (3.1) and integrating both sides in a similar computation with the first item in case to, we get

$$u(\eta) = \psi(\eta) = r_8 + A_3 - \frac{2A_3}{1 - \mathrm{cn}(\Omega_6\eta, k_5)}, \quad 0 < \eta < \eta_4, \tag{3.15}$$

where $\Omega_6 = \frac{\sqrt{2A_3}}{k}, k_5 = \sqrt{\frac{A_3 - \Re c_3 + r_8}{2A_3}}, A_3^2 = [\Re c_3 - r_8]^2 + \Im^2 c_3$ and $\eta_4 = \frac{4}{\Omega_6}K(k_5)$, where $K(k_5)$ is a complete elliptic integral of the first type [2].

4. On the level of the energy corresponding to the saddle point E_3, i.e., $h = h_3$, there is an orbit in red as clarified by Fig. 1(b). This orbit consists of two parts; the first is a homoclinic orbit which is considered in sub subsection 3.1.2. While the the second is its extension and it will be considered here. The polynomial $R_3(\psi)$ takes the form $R_3(\psi) = (\psi - r_4)^2(r_5 - \psi)$, where $-\infty < \psi < r_4 < r_5$ and assume $\psi(0) = -\infty$. Using the last expression for R_3 and Eq. (3.1) and integrating both sides, we get

$$\int_{-\infty}^{\psi} \frac{dq}{(r_4-q)\sqrt{r_5-q}} = \frac{\sqrt{2}}{k}\int_0^{\eta} d\eta, \tag{3.16}$$

for $\eta > 0$. It follows that

$$u(\eta) = \psi(\eta) = r_5 + \frac{2(r_5 - r_4)}{1 - \cosh\Omega_7\eta}, \quad \eta > 0, \tag{3.17}$$

where $\Omega_7 = \frac{\sqrt{2(r_5-r_4)}}{k}$.

5. On the energy level which equals the value of the energy at the center point E_2, i.e. $h = h_2$, the system (2.5) has a unbounded orbit in black in addition to Equilibrium point E_2. Thus, the polynomial $R_3(\psi)$ takes the form $R_3(\psi) = (\psi - r_{10})^2(r_9 - \psi)$, where $r_9 < r_{10} = \frac{-\gamma k^2 + k\sqrt{\gamma^2 k^2 + 12\rho}}{6}$ and $-\infty < \psi < r_9$. Assume $\psi(0) = -\infty$, entering the last expression for $R_3(\psi)$ into Eq. (3.1), and integrate both sides, we get

$$\int_{-\infty}^{\psi} \frac{dq}{(r_{10}-q)\sqrt{r_9-q}} = \frac{\sqrt{2}}{k}\int_0^{\eta} d\eta, \tag{3.18}$$

for $\eta > 0$. It follows that

$$u(\eta) = \psi(\eta) = r_{10} - \frac{2(r_{10} - r_9)}{1 + \sin \Omega_8 \eta}, \quad \eta > 0, \tag{3.19}$$

where $\Omega_8 = \frac{\sqrt{2(r_{10} - r_9)}}{k}$.

Case 3.3: If $(\rho, k, \gamma) \in \mathcal{C}_-$, then the dynamical system (2.5) has no equilibrium point and its phase portrait is clarified by Fig. 1(c). All orbits are unbounded and each one of them intersects $\psi-$ axis in one point. This shows $R_3(\psi)$ has one real root and two complex roots and hence, it takes the form $R_3(\psi) = (r_{11} - \psi)(\psi - c_4)(\psi - \bar{c_4})$, where $-\infty < \psi < r_{11}$. We assume $\psi(-\infty) = 0$, insert the last expression for $R_3(\psi)$ into Eq. (3.1), and integrate both sides, we obtain

$$u(\eta) = \psi(\eta) = r_{11} + A - \frac{2A}{1 - cn(\Omega_9 \eta, k_6)}, \qquad 0 < \eta < \eta_5, \tag{3.20}$$

where $\Omega_9 = \frac{\sqrt{2A}}{k}$, $k_6 = \sqrt{\frac{A + r_{11} - \Re c_4}{2A}}$, $A_4^2 = [\Re c_4 - r_{11}]^2 + \Im^2 c_4$, and $\eta_5 = \frac{2}{\Omega_9} K(k_6)$. The solution (3.20) is new traveling wave solution for Eq. (1.1).

4. Graphic representation

This section pursues to illustrate some wave solutions by displaying 3D graphics to them, the corresponding orbit of this solution, in addition to the density diagram.

For $k = 1, \gamma = 2, \rho = 1$, the dynamical system (2.5) has two equilibrium points $E_2 = (\frac{1}{3}, 0), E_3 = (-1, 0)$ and notice the type of the orbit depends on the value of h as it was discussed in section 2. Let us clarify that for different values of h:

- if $h = 0.5$ which lies between the values of the energy at the two equilibrium points E_2 and E_3, then the system (2.5) has an orbit as outlined by Fig. 3(a). This orbit consists of two parts; the first one is closed periodic orbit and corresponds to the periodic solution (3.5) clarified by Fig. 3(b) with the density diagram explained by Fig. 3(c). The second one, which takes the shape of a parabola, corresponds to the solution (3.14) which is clarified by Fig. 4(a) with the density diagram outlined by Fig. 4(b).

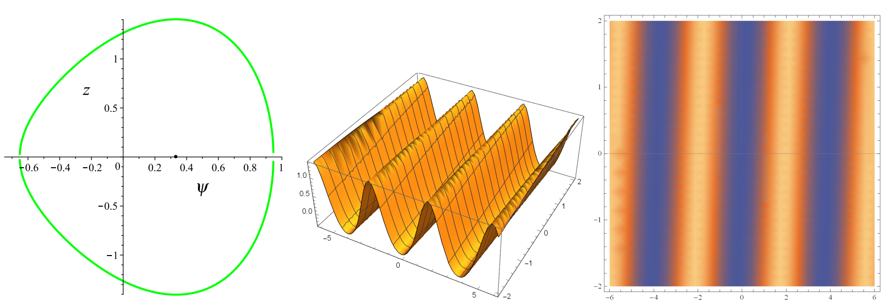

(a) 2D-Graphic (b) 3D-Graphic (c) Density Plot

Figure 3. Graphic representations for the periodic solution (3.5).

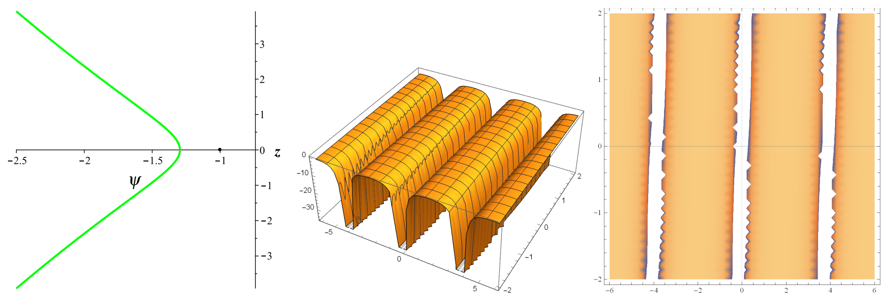

(a) 2D-Graphic (b) 3D-Graphic (c) Density Plot

Figure 4. Graphic representations for the solution (3.14).

- When $h = 1$ which is the energy at the equilibrium point $E_3 = (-1, 0)$, the dynamical system (5) has an orbit consisting of two parts: The first one is a homoclinic orbit connecting the saddle point E_3, around the center E_2, with itself as in Fig. 5 (a). This orbit corresponds to the solitary solution (3.7) outlined by Fig. 5(b) with the density diagram shown by Fig. 5(c). The second one is the extension of the homoclinic orbit and it corresponds to the singular solution (3.17). This solution and its density diagram are shown by Fig. 6(a) and (b).

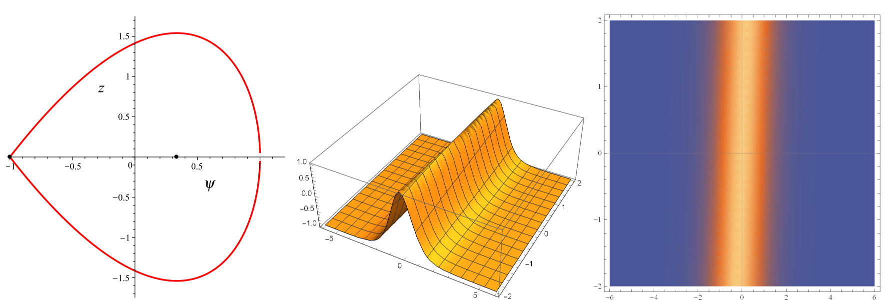

(a) 2D-Graphic (b) 3D-Graphic (c) Density Plot

Figure 5. Graphic representations for the solitary solution (3.7).

For $k = 1, \gamma = -6, \rho = -3$, the dynamical system (2.5) has a unique equilibrium point $E_1 = (1, 0)$ which is a cusp. We clarify the wave solution and its corresponding orbit for different values of h:

- On the energy $h = 1$ of the cusp point, the dynamical system (2.5) has an orbit shown by Fig. 7(a). This orbit corresponds to the solution (3.10) outlined by Fig. 7(b) with the density diagram displayed by Fig. 7(c).
- On any other level of energy, the system (2.5) has two types of orbits depending on whether $h > 1$ (blue orbit) or $h < 1$ (brown orbit), see Fig. 8(a). Thus, when $h = 2$, the solution (3.9) is outlined by Fig. 8(b) with the density diagram displayed by Fig. 8(c).

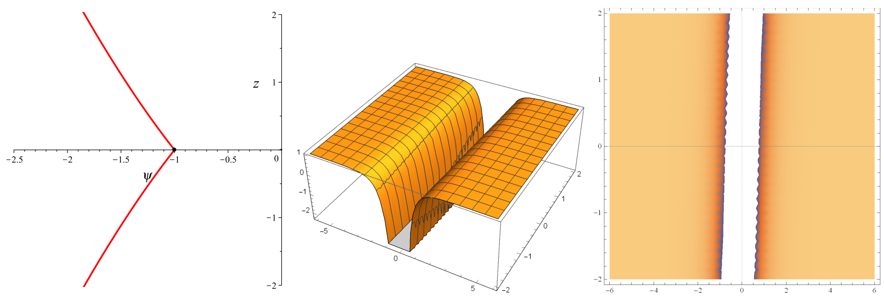

(a) 2D-Graphic (b) 3D-Graphic (c) Density Plot

Figure 6. Graphic representations for the solution (3.17).

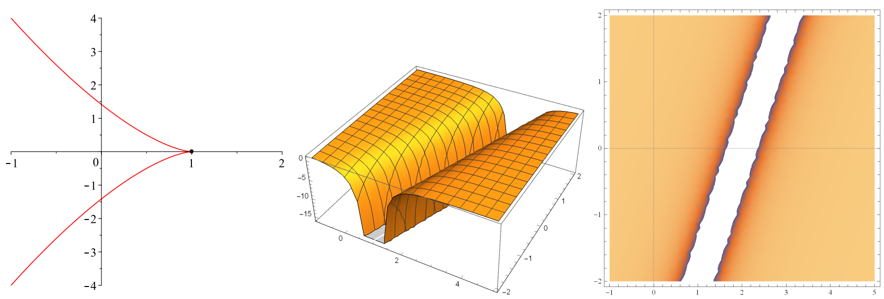

(a) 2D-Graphic (b) 3D-Graphic (c) Density Plot

Figure 7. Graphic representations for the solution (3.10).

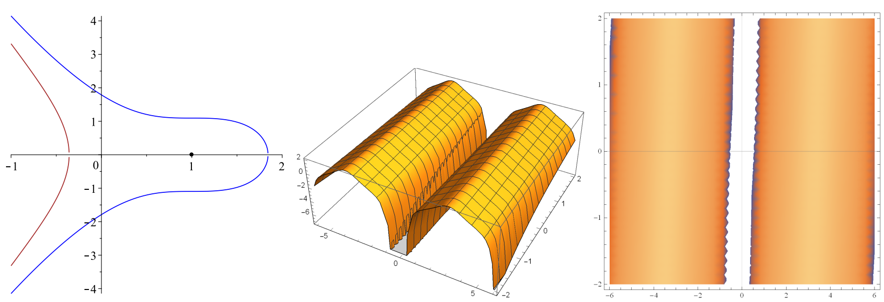

(a) 2D-Graphic (b) 3D-Graphic (c) Density Plot

Figure 8. Graphic representations for the solution (3.9).

5. Quasi-Periodic solutions

This section aims to examine the dynamical behaviour of the perturbed form of Eq. (1.1) as a result of adding the perturbed periodic term $A\cos(q(kx+ly-\omega t))$, where A, q are arbitrary constants. Hence, Eq. (1.1) takes the form

$$(u_t+6uu_x+u_{xxx})_x-u_{yy}+\alpha u_{tt}+\beta u_{ty}+A\cos(q(kx+ly-\omega t))=0. \tag{5.1}$$

Applying the transformation (2.1) to Eq. (1.1), integrating twice with respect to η and setting the first integration constant equals zero, we obtain

$$\psi'' + \frac{3}{k^2}\psi^2 + \gamma\psi - p\cos(q\eta) = \rho, \tag{5.2}$$

where $p = \frac{A}{q^2}$. Eq. (5.2) can be written as a $2D$- non autonomous dynamical system in the form

$$\begin{aligned} \psi' &= z, \\ z' &= \frac{-3}{k^2}\psi^2 - \gamma\psi + \rho + p\cos(q\eta). \end{aligned} \tag{5.3}$$

In order to look for some distinct dynamical behaviours of the perturbed Eq. (1.1), we investigate several values of the physical parameters. Fig. 9 illustrates the $2D$ and $3D$ phase portrait for the perturbed dynamical system (5.3) when the system's parameters takes the values $k = 1, p = -0.05, q = 2, \rho = -1, \gamma = 1$ with initial conditions $\psi(0) = 0.05, z(0) = 0.05$. While, Fig. 10 clarifies the $2D$ and $3D$ phase portrait for the perturbed dynamical system (5.3) when the parameters of the system admits the values $k = 0.04, p = 5, q = 0.05, \rho = 4, \gamma = 2$ with initial conditions $\psi(0) = 0.05, z(0) = 1$. Consequently, the perturbed dynamical system (5.3) is observed to have quasi- periodic behaviours as outlined by the two Figs. 9 and 10.

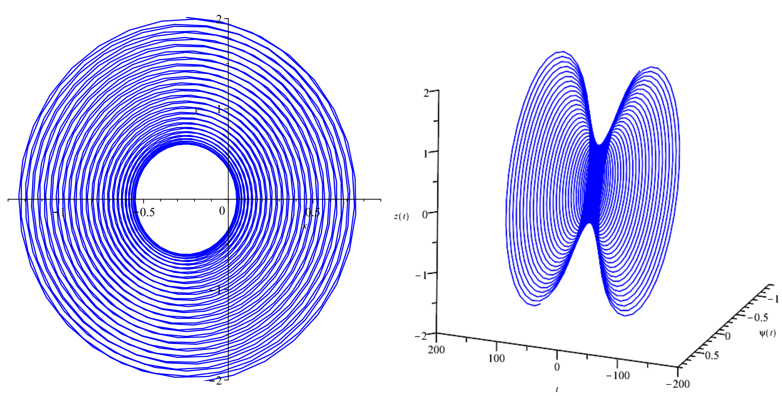

(a) 2D-phase portrait

(b) 3D-phase portrait

Figure 9. Phase portrait for the dynamical system (5.3) when $k = 1, p = -0.05, q = 2, \rho = -1, \gamma = 1$, and $\psi(0) = 0.05, z(0) = 0.05$.

6. Conclusion

We have interested in studying a (2+1)-dimensional extended Kadomtsev–Petviashvili equation. We have applied a well-known wave transformation to convert Eq. (1.1) into a second order differential equation which is rewritten as a two dimensional dynamical system. This system has been proven to be a conservative Hamiltonian system having a conserved quantity. The bifurcation analysis and phase portrait for the Hamilton system have been investigated. We have been motivated by the applying the bifurcation method due to the following reasons:

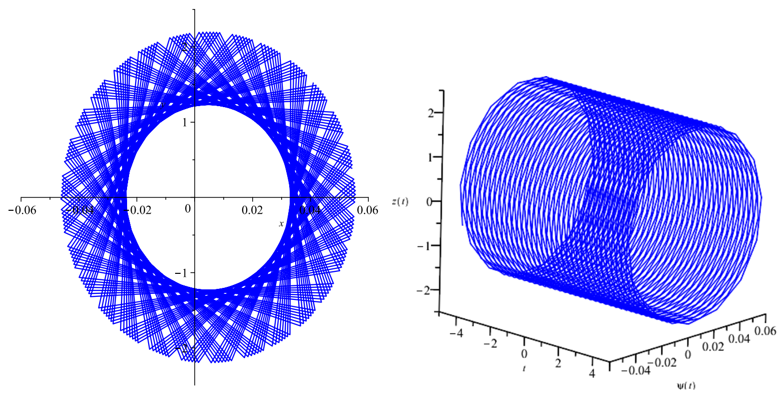

(a) 2D-phase portrait (b) 3D-phase portrait

Figure 10. Phase portrait for the dynamical system (5.3) when $k = 0.04, p = 5, q = 0.05, \rho = 4, \gamma = 2$, and $\psi(0) = 0.05, z(0) = 1$.

(a) The bifurcation analysis enables us to determine the type of the wave solution via the type of the orbits. This is clear form proposition 3.1, the Hamilton system (2.5) has only periodic and homoclinic orbits see, Fig. 1(b) while the other orbits are unbounded Fig. 1(a), (c). Hence, this proves the equation under consideration (1.1) has periodic and solitary wave solutions beside unbounded wave solutions corresponding to unbounded orbits.

(b) The integration of both sides of Eq. (3.1) requires the range of the included parameters to find all possible solutions. Based on this range of the parameter, we determine the allowed interval for real propagation. Sometimes, there are several region of real propagation for the same range of the parameters leading to completely different solutions. Let us clarify that. If $(\rho, k, \gamma) \in \mathcal{C}_+$ and $h \in]h_2, h_3[$, the dynamical system (2.5) has an orbit in green as outlined by Fig. 1(b). This orbit consists of two parts. The first one is bounded periodic orbit and the corresponding solution is (3.5) which is periodic solution. The second part is unbounded and hence, the corresponding solution is (3.14) which is singular solution. Thus, for the same conditions, we have two completely different solutions from the mathematical and physical point of view, see Table.1.

Table 1. Conditions on the parameters and permitted interval of real propagation

No.	Conditions on the parameters	Interval of real propagation	Solution and its type	Figures
1	$(\rho, \varphi, k) \in \mathcal{C}_+$,	(a) $r_2 < \psi < r_3$	(a) Eq. (3.5), periodic	Fig. 3
	$h \in]h_2, h_3[$	(b)$-\infty < \psi < r_1$	(b)Eq. (3.14), Singular	Fig. 4
2	$(\rho, \varphi, k) \in \mathcal{C}_+$,	(a) $r_4 < \psi < r_5$	(a) Eq. (3.7), Solitary	Fig. 5
	$h = h_3$	(b)$-\infty < \psi < r_4$	(b) Eq. (3.17), Singular	Fig. 6

Employing the conserved quantity, new traveling wave solutions that are classified into periodic, solitary, and singular solutions have been constructed and explained graphically. Finally, the dynamical behavior of a perturbed form of the equation has been investigated by adding the perturbed periodic cosine term.

Conflict of interest

The authors declare that the research was conducted in the absence of any conflict of interest.

Acknowledgements

The authors acknowledge the Deanship of Scientific Research at King Faisal University for the financial support under Nasher Track (No. 206139).

References

[1] I. Ahmed, A. R. Seadawy and D. Lu, *Mixed lump-solitons, periodic lump and breather soliton solutions for (2+1)-dimensional extended Kadomtsev-Petviashvili dynamical equation*, International Journal of Modern Physics B, 2019, 33(05), 1950019. DOI: 10.1142/S021797921950019X.

[2] P. F. Byrd and M. D. Fridman, *Handbook of elliptic integrals for engineers and scientists*, Berlin: Springer, 1971.

[3] S. Beji, *Kadomtsev-Petviashvili type equation for entire range of relative water depths*, Coastal engineering journal, 2018, 60(1), 60–68. DOI:10.1080/21664250.2018.1436241.

[4] A. Biswas, *1-Soliton solution of the generalized Camassa-Holm Kadomtsev-Petviashvili equation*, Communications in Nonlinear Science and Numerical Simulation, 2009, 14(6), 2524–2527. DOI: 10.1016/j.cnsns.2008.09.023.

[5] A. H. Bhrawy, M. A. Abdelkawy, S. Kumar and A. Biswas, *Solitons and other solutions to Kadomtsev-Petviashvili equation of B-type*, Romanian Journal of Physics, 2013, 58(7), 729–748.

[6] L. Cheng and Y. Zhang, *Multiple wave solutions and auto- Bäcklund transformation for the (3+1)-dimensional generalized B-type Kadomtsev-Petviashvili equation*, Computers and Mathematics with Applications, 2015, 70(5), 765–775. DOI: 10.1016/j.camwa.2015.05.028.

[7] P. Dubard and V. B. Matveev, *Multi-rogue waves solutions: from the NLS to the KP-I equation*, Nonlinearity, 2013, 26(12), R93. DOI: 10.1088/0951-7715/26/12/R93.

[8] M. Darvishi, M. Najafi, S. Arbabi and L. Kavitha, *Exact propagating multi-anti-kink soliton solutions of a (3+1)-dimensional B-type Kadomtsev-Petviashvili equation*, Nonlinear Dynamics, 2016, 83(3), 1453–1462. DOI: 10.1007/s11071-015-2417-2.

[9] G. Ebadi, N. Y. Fard, H. Triki and A. Biswas, *Exact solutions of the (2+1)-dimensional Camassa-Holm Kadomtsev-Petviashvili equation*, Nonlinear Analysis: Modelling and Control, 2012, 17(3), 280–296.

[10] G. Ebadi, A. H. Kara, M. D. Petkovic, A. Yildirim and A. Biswas, *Solitons and conserved quantities of the Ito equation*, Proceedings of the Romanian Academy: Series A, 2012, 13, 215–224.

[11] G. Ebadi, N. Y. Fard, A. H. Bhrawy, S. Kumar, H. Triki, A. Yildirim and A. Biswas, *Solitons and other solutions to the (3+1)-dimensional extended Kadomtsev-Petviashvili equation with power law nonlinearity*, Romanian Reports in Physics, 2013, 65, 27–62.

[12] K. El-Rashidy, A. R. Seadawy, S. Althobaiti and M. M. Makhlouf, *Multiwave, Kinky breathers and multi-peak soliton solutions for the nonlinear Hirota dynamical system*, Results in Physics, 2020, 19, 103678. DOI: 10.1016/j.rinp.2020.103678.

[13] K. El-Rashidy, *New traveling wave solutions for the higher Sharma-Tasso-Olver equation by using extension exponential rational function method*, Results in Physics, 2020, 17, 103066. DOI: 10.1016/j.rinp.2020.103066.

[14] K. El-Rashidy and A. R. Seadawy, *Kinky breathers, multi-peak and multi-wave soliton solutions for the nonlinear propagation of Kundu–Eckhaus dynamical model*, International Journal of Modern Physics B, 2020, 34(32), 2050317. DOI: 10.1142/S0217979220503178.

[15] K. El-Rashidy, A. R. Seadawy, S. Althobaiti and M. M. Makhlouf, *Investigation of interactional phenomena and multi wave solutions of the quantum hydrodynamic Zakharov–Kuznetsov model*, Open Physics, 2021, 19(1), 91–99. DOI: 10.1515/phys-2021-0009.

[16] A. A. Elmandouh and A. G. Ibrahim, *Bifurcation and travelling wave solutions for a (2+1)-dimensional KdV equation*, Journal of Taibah University for Science, 2020, 14 (1), 139–147. DOI: 10.1080/16583655.2019.1709271.

[17] A. A. Elmandouh, *Bifurcation and new traveling wave solutions for the 2D Ginzburg–Landau equation*, European Phyical Journal Plus, 2020, 135, 648. DOI: 10.1140/epjp/s13360-020-00675-3.

[18] M. E. Elbrolosy and A. A. Elmandouh, *Bifurcation and new traveling wave solutions for (2+1)-dimensional nonlinear Nizhnik–Novikov–Veselov dynamical equation*, European Phyical Journal Plus, 2020, 135, 533. DOI: 10.1140/epjp/s13360-020-00546-x.

[19] M. E. Elbrolosy and A. A. Elmandouh, *Dynamical behaviour of nondissipative double dispersive microstrain wave in the microstructured solids*, The European Physical Journal Plus, 2021, 136(9), 1–20. DOI: 10.1140/epjp/s13360-021-01957-0.

[20] M. E. Elbrolosy, *Qualitative analysis and new soliton solutions for the coupled nonlinear Schrödinger type equations*, Physica Scripta, 2021. DOI: 10.1088/1402-4896/ac445c.

[21] A. A. Elmandouh, *Integrability, qualitative analysis and the dynamics of wave solutions for Biswas–Milovic equation*, The European Physical Journal Plus, 2021, 136(6), 1–17. DOI: 10.1140/epjp/s13360-021-01626-2.

[22] J. Guo, J. He, M. Li and D. Mihalache, *Exact solutions with elastic interactions for the (2+1)-dimensional extended Kadomtsev-Petviashvili Equation*, Nonlinear Dynamics, 2020, 101, 2413–2422. DOI: 10.1007/s11071-020-05881-3.

[23] X. Guan and W. Liu, *Multiple-soliton and lump-kink solutions for a generalized (3+1)-dimensional Kadomtsev-Petviashvili equation*, Results in Physics, 2020, 17, 103149. DOI: 10.1016/j.rinp.2020.103149.

[24] A. J. M. Jawad, *Dynamics of shallow water waves with Gardner-Kadomtsev-Petviashvili equation*, Discrete and continuous dynamical systems series S, 2015, 8(6), 1155–1164. DOI: 10.3934/dcdss.2015.8.1155.

[25] J. Liu and Z. Zeng, *Auto- Bäcklund transformation and new exact solutions of the (3+1)-imensional KP equation with variable coefficients*, Journal of Theoretical and Applied Physics, 2013, 7, 49. DOI: 10.1186/2251-7235-7-49.

[26] J. Li, Y. Zhang and J. Liang, *Bifurcation and exact traveling wave solutions for a new integrable non-local equation*, Journal of Applied Analysis and Computation, 2021, 11(3), 1588–1599. DOI: 10.11948/20200319.

[27] Q. Meng and B. He, *Bifurcation analysis and exact traveling wave solutions for a generic two-dimensional sine-Gordon equation in nonlinear optics*, Journal of Applied Analysis and Computation, 2020, 10(4), 1443–1463. DOI: 10.11948/20190227.

[28] W. Mao, *Bifurcation and exact traveling wave solutions of MN-Wang equation*, Journal of Applied Analysis and Computation, 2020, 10(1), 210–222. DOI: 10.11948/20190113.

[29] W. Ma, *Lump solutions to the Kadomtsev-Petviashvili equation*, Physics Letters A, 2015, 379(36), 1975–1978. DOI: 10.1016/j.physleta.2015.06.061.

[30] S. Manukure, Y. Zhou and W. Ma, *Lump solutions to a (2+1)-dimensional extended KP equation*, Computers and Mathematics with Applications, 2018, 75(7), 2414–2419. DOI: 10.1016/j.camwa.2017.12.030.

[31] M. A. Nuwairan and A. A. Elmandouh, *Qualitative analysis and wave propagation of the nonlinear model for low-pass electrical transmission lines*, Physica Scripta, 2021, 96(9), 095214. DOI: 10.1088/1402-4896/ac0989.

[32] J. Song and J. Li, *Bifurcations and exact travelling wave solutions for a shallow water wave model with a non-stationary bottom surface*, Journal of Applied Analysis Computation, 2020, 10(1), 350–360. DOI: 10.11948/20190254.

[33] A. R. Seadawy and K. El-Rashidy, *Dispersive solitary wave solutions of Kadomtsev-Petviashvili and modified Kadomtsev-Petviashvili dynamical equations in unmagnetized dust plasma*, Results in Physics 8, 2018, 1216–1222. DOI: 10.1016/j.rinp.2018.01.053.

[34] Y. Sun, W. Ma, J. Yu and C. M. Khalique, *Dynamics of lump solitary wave of Kadomtsev-Petviashvili-Boussinesq-like equation*, Computers and Mathematics with Applications, 2019, 78(3), 840–847. DOI: 10.1016/j.camwa.2019.03.001.

[35] A. R. Seadawy, M. Iqbal and D. Lu, *Propagation of long-wave with dissipation and dispersion in nonlinear media via generalized Kadomtsive-Petviashvili modified equal width Burgers equation*, Indian Journal of Physics, 2020, 94(5), 675–687. DOI: 10.1007/s12648-019-01500-z.

[36] H. Triki, S. Crutcher, A. Yildirim, T. Hayat, O. M. Aldossary and A. Biswas, *Bright and dark solitons of the modified complex Ginzburg Landau equation with parabolic and dual-power law nonlinearity*, Romanian Reports in Physics, 2012, 64, 367–380.

[37] H. Triki, A. Yildirim, T. Hayat, O. M. Aldossary and A. Biswas, *Topological and non-topological soliton solutions of the bretherton equation*, Romanian Reports in Physics, 2012, 64, 672–684.

[38] Y. Wang and J. Deng, *Explicit solutions and conservation laws of the logarithmic-KP equation*, Advances in Difference Equations, Article number 229, 2016, DOI: 10.1186/s13662-016-0948-6.

[39] H. Wang, *Solitons of the Kadomtsev-Petviashvili equation based on lattice Boltzmann model*, Advances in Space Research, 2017, 59(1), 293–301. DOI: 10.1016/j.asr.2016.08.029.

[40] A. M. Wazwaz, *Multiple-soliton solutions for the KP equation by Hirota's bilinear method and by the tanh-coth method*, Applied Mathematics and Computation, 2007, 190(1), 633–640. DOI: 10.1016/j.amc.2007.01.056.

[41] A. M. Wazwaz, *Two integrable extensions of the Kadomtsev-Petviashvili equation*, Central European Journal of Physics, 2011, 91, 49–56. DOI: 10.2478/s11534-010-0056-2.

[42] A. M. Wazwa, *Extended KP equations and extended system of KP equations: multiple-soliton solutions*, Canadian Journal of Physics, 2011, 89(7), 739–743. DOI: 10.1139/p11-065.

[43] A. M. Wazwaz, *Gaussian solitary waves for the logarithmic-KdV and the logarithmic-KP equations*, Physica Scripta, 2014, 89(9), 095206. DOI: 10.1088/0031-8949/89/9/095206.

[44] S. Xie, L. Wang and Y. Zhang, *Explicit and implicit solutions of a generalized Camassa-Holm Kadomtsev-Petviashvili equation*, Communications in Nonlinear Science and Numerical Simulation, 2012, 17(3), 1130–1141. DOI: 10.1016/j.cnsns.2011.07.003.

[45] Z. Xu, H. Chen, M. Jiang, M. Dai and W. Chen, *Resonance and deflection of multi-soliton to the (2+1)-dimensional Kadomtsev-Petviashvili equation*, Nonlinear Dynamics, 2014, 78, 461–466, DOI: 10.1007/s11071-014-1452-8.

[46] J. Yu and Y. Sun, *Study of lump solutions to dimensionally reduced generalized KP equations*, Nonlinear Dynamics, 2017, 87, 2755–2763. DOI: 10.1007/s11071-016-3225-z.

[47] J. Zhuang and Y. Zhou, *Bifurcation and exact traveling wave solutions of the equivalent complex short-plus equations*, Journal of Applied Analysis Computation, 2020, 10(2), 795–815. DOI: 10.11948/20190408.